ELSEVIER

Catalysis Today 35 (1997) 435–442

CATALYSIS TODAY

Effect of the wall Nusselt number on the simulation of catalytic fixed bed reactors

Olaf R. Derkx [1], Anthony G. Dixon [*]

Department of Chemical Engineering, Worcester Polytechnic Institute, 100 Institute Road, Worcester MA 01609, USA

Abstract

Literature correlations for the apparent wall heat transfer coefficient (h_w) in fixed bed catalytic reactors are compared. At low to moderate values of the Reynolds number (Re), different correlations can produce estimates of the dimensionless wall Nusselt number ($Nu_w = h_w d_p/k_f$) that differ by an order of magnitude or more. Some correlations give Nu_w as a function of Re only, others allow for the effects of tube-to-particle diameter ratio and particle and fluid thermal conductivities. The value of Nu_w that is used in a simulation of a fixed bed catalytic reactor can have a strong effect on the predicted behavior. Two examples of fixed bed reactors are simulated and show that the more general correlations for Nu_w are to be preferred.

Keywords: Fixed bed reactor; Wall heat transfer coefficient; Wall Nusselt number; Packed beds

1. Introduction

Heat transfer in fixed beds is a very important topic for the chemical engineer because fixed beds are widely used in the chemical industry, as reactors, thermal storage devices and contacting units for adsorption and absorption. The radial heat transfer in a wall-cooled fixed bed reactor is determined by resistances in series. There is a resistance to heat transfer through the bed, a resistance in the wall, and a resistance from the wall to the coolant. Frequently, significant radial temperature gradients exist in the bed, which are commonly described in a pseudohomogeneous model by an effective radial thermal conductivity k_r.

Experimental data, however, show a temperature jump near the wall. A typical example from a laboratory fixed-bed heat exchanger is shown in Fig. 1. Apparently there is an extra resistance to heat transfer near the wall, and this cannot be described by models using a constant value of k_r. In the literature there is still not a consensus about this extra resistance. A literature survey by Vortmeyer and Haidegger [1] reveals that the majority of researchers still favour the wall heat transfer coefficient approach of Coberly and Marshall [2]:

$$q_r = h_w\left(T|_{r=R} - T_w\right) \tag{1}$$

In this equation, the radial heat flux q_r at the wall is evaluated by a temperature jump at the wall in combination with a wall heat transfer coefficient. The quantity $1/h_w$ represents the extra resistance to heat transfer *near* the wall, which has been idealized to be an extra resistance *at* the wall.

[*] Corresponding author.

[1] Presently with DSM, Geleen, The Netherlands.

PII S0920-5861(96)00210-6

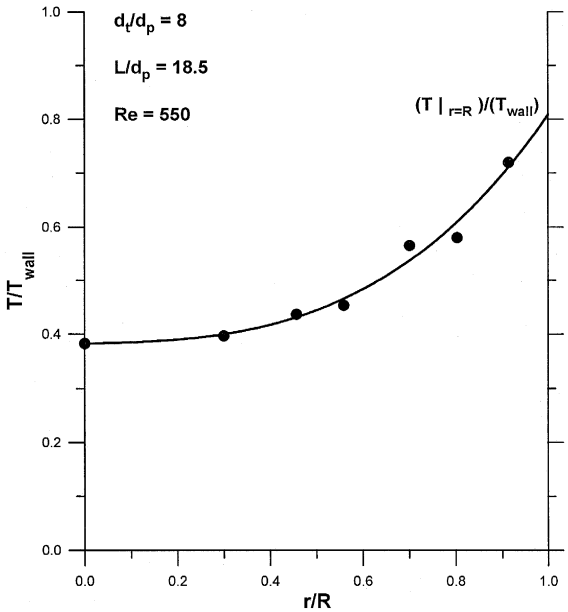

Fig. 1. Typical radial temperature profile in a wall-heated fixed bed laboratory apparatus.

Much has been published in the literature about the wall heat transfer coefficient in fixed beds, however, there is still no general agreement about it. There is discussion about the real meaning of this coefficient, about the range of applicability and, most importantly, about how this quantity can be predicted [3]. Although the concept of this model is simple and appealing, the behavior of wall heat transfer coefficients gained by comparison of the model with measurements is quite discouraging [3,4]. In the operating range of fixed bed reactors (Reynolds numbers between 100 and 5000), experimental data show that there appears to be no unique correlation between the wall heat transfer coefficient h_w, expressed in terms of a wall Nusselt number Nu_w, and the gas velocity, expressed in terms of a Reynolds number, *Re*.

Many researchers state that there should be a unique correlation between the two [1],[3],[5–7]. Some of these authors refer to the wide spread in the measured values of Nu_w as experimental error or scatter, others [5,6] explain that not all data points are independent of the length and claim that the so-called scatter is caused by the fact that different researchers use different techniques to measure the temperature profiles in fixed beds. Some researchers show that, theoretically, there is not supposed to be such a unique correlation [8,9].

Disagreements between predicted and measured fixed bed reactor performance have led some researchers to consider complex reactor models [1]. Some of the features that have been introduced by different workers include axial conduction, non-uniform velocity profiles, non-uniform porosity and thermal conductivity and conduction along the reactor wall. It is questionable whether these phenomena are important for the reactor simulation, or whether the failure of models to predict in some cases is attributable to some other cause.

Clearly there is a need to resolve this issue, because the engineer who has to design a fixed bed reactor must choose a model or correlation for predicting correct values of the heat transfer parameters, so that he or she is able to simulate a reaction based on these heat transfer parameters and compare the results with experimental data. He or she is faced with an enormous choice of conflicting results with no clear criteria available for guidance [10]. In this paper, the two existing approaches for correlating wall heat transfer coefficients in fixed bed reactors will be compared. The wall heat transfer coefficient will be predicted with two representative correlations, and applied in two reactor simulation examples. The differences in simulated behavior will be used to discriminate between correlations for Nu_w, and to draw some conclusions on the need for complicated reactor models.

2. Wall heat transfer coefficient correlations

The wall heat transfer coefficient h_w is often correlated as a function of Re^n in analogy with the wall heat transfer coefficient in an empty tube. Li and Finlayson [5] reviewed and brought together a lot of experimental heat transfer data

from prior researchers. They stated that the wall heat transfer coefficient depends on length and that this length dependency becomes less prominent with increasing Reynolds number. They re-examined all data in order to exclude studies that they considered were influenced by the length effect, and from a best fit to the remaining data they suggested the following correlation for spherical packings:

$$Nu_w = 0.17\,Re^{0.79}.$$

Li and Finlayson reported this correlation to be valid for $20 < Re < 7600$ and a tube-to-particle diameter ratio $3.3 < d_t/d_p < 20$. Their correlation does not have any material thermal conductivity dependency nor does it have any tube-to-particle diameter ratio dependency.

Dixon and Cresswell [8] presented a model matching approach that takes both solid and fluid phase heat transfer mechanisms into account. Their earlier results were extended [11] and are recast here in terms of theoretical predictions of Nu_w and the effective radial thermal conductivity k_r:

High Re

$$\frac{k_r}{k_f} = \frac{RePr}{Pe_{rf}} + \beta_s \frac{Bi_f + 4}{Bi_f},$$

$$Nu_w = \frac{8\beta_s}{d_t/d_p} + Nu_{wf}\left(1 + \beta_s \frac{Pe_{rf}}{RePr}\right), \quad (3)$$

where

$$\beta_s = \frac{k_{rs}/k_f}{\frac{8}{N_s} + \frac{Bi_s + 4}{Bi_s}}, \quad (4)$$

and

$$N_s = \frac{1.5(1-\epsilon)(d_t/d_p)^2}{\frac{k_{rs}}{k_f}\left[\frac{1}{Nu_{fs}} + \frac{0.1}{k_p/k_f}\right]}. \quad (5)$$

Low Re

$$\frac{k_r}{k_f} = \frac{k_{rs}}{k_f} + \beta_f \frac{Bi_s + 4}{Bi_s},$$

$$Nu_w = \frac{8\beta_f}{d_t/d_p} + 2\,Bi_s \frac{k_{rs}}{k_f}\frac{d_p}{d_t}\left(1 + \frac{\beta_f}{k_{rs}/k_f}\right), \quad (6)$$

where

$$\beta_f = \frac{(RePr)/Pe_{rf}}{\frac{8}{N_f} + \frac{Bi_f + 4}{Bi_f}}, \quad (7)$$

and

$$N_f = \frac{1.5(1-\epsilon)(d_t/d_p)^2}{\frac{RePr}{Pe_{rf}}\left[\frac{1}{Nu_{fs}} + \frac{0.1}{k_p/k_f}\right]}. \quad (8)$$

These formulas give the lumped parameters k_r/k_f and Nu_w in terms of the more fundamental parameters for the individual phases and the interphase heat transfer coefficient. These parameters may be independently determined from experiments designed to isolate the transport

Table 1
Single-phase heat transfer correlations for use in the extended Dixon/Cresswell parameter relations

Single-phase parameter	Correlation	Reference
Nu_{wf}	$Nu_{wf} = 0.523(1 - \frac{d_p}{d_t})Pr^{0.33}Re^{0.738}$	[17]
Bi_s	$Bi_s = 2.41 + 0.156(\frac{d_t}{d_p} - 1)^2$	[11]
k_{rs}/k_f	$\frac{k_{rs}}{k_f} = \frac{\bar{k}_{rs}}{k_f}(\frac{Bi_s + 4}{Bi_s})$	[18,19]
	$\frac{\bar{k}_{rs}}{k_f} = f(\epsilon, k_p/k_f)$	
Pe_{rf}	$\frac{1}{Pe_{rf}} = \frac{1}{Pe_{rf}(\ )} + \frac{\epsilon\tau}{RePr}$	[20,21]
	$Pe_{rf}(\ ) = 7(2 - (1\frac{d_p}{d_t})^2)$	
Nu_{fs}	$Nu_{fs} = 2.0 + 1.1\,Pr^{0.33}Re^{0.6}$	[22]

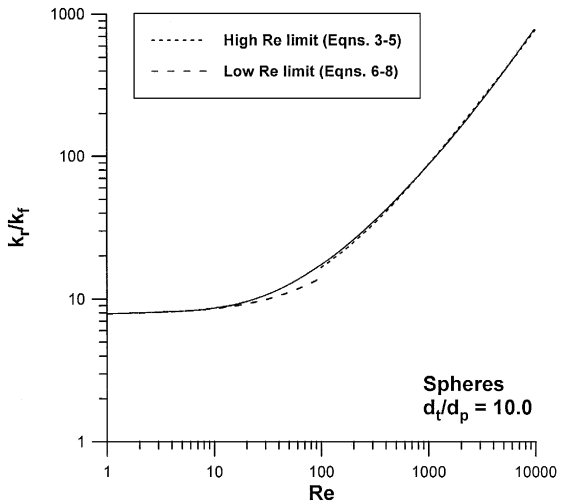

Fig. 2. Predicted effective thermal conductivity using extended theory of Dixon and Cresswell [8,11].

mechanisms, for example by analogy with mass transfer experiments in which only the fluid phase contributes, and from stagnant bed experiments in which solid phase conduction predominates. The correlations used in the present work for these individual transport parameters are listed in Table 1.

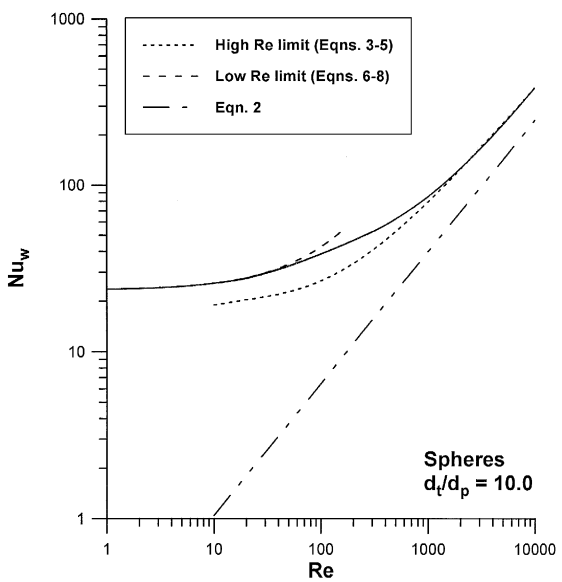

Fig. 3. Comparison of predictions for Nu_w using correlation of Li and Finlayson [5] and extended theory of Dixon and Cresswell [8,11].

Eqs. (3)–(8) are depicted in Fig. 2 and Fig. 3 for a typical case of a ceramic, spherical catalyst packing with a d_t/d_p ratio of ten. An interpolating curve has been drawn for each case between the two limiting curves. In Fig. 3, Eq. (2) has also been included for comparison. Some more recent papers [7,9] have also formulated approaches along the same lines, with empirical fits to their own or others data.

3. Reactor model equations

The object of the present work is to compare the effects of different correlations for Nu_w, so a standard pseudohomogeneous two-dimensional model was chosen [12], with axial dispersion and conduction neglected. No attempt was made to evaluate the necessity for a heterogeneous model in the reaction examples analyzed here. The model equations are:

$$\frac{\partial X_A}{\partial z} = \frac{d_p}{Pe_{rm}}\left(\frac{\partial^2 X_A}{\partial r^2} + \frac{1}{r}\frac{\partial X_A}{\partial r}\right) + \frac{r(X_A,T)}{(Gy_{A0}/M_0)}, \tag{9}$$

and

$$\frac{\partial T}{\partial z} = \frac{d_p}{Pe_{rh}}\left(\frac{\partial^2 T}{\partial r^2} + \frac{1}{r}\frac{\partial T}{\partial r}\right) + \frac{(-\Delta H_R)r(X_A, T)}{(G\hat{c}_p)}, \tag{10}$$

with initial conditions

$$X_A(0) = 0,$$
$$T(0) = T_0, \tag{11}$$

and boundary conditions

$$\frac{\partial X_A}{\partial r}(r=0) = 0,$$
$$\frac{\partial X_A}{\partial r}(r=R) = 0,$$

$$\frac{\partial T}{\partial r}(r=0)=0,$$

$$\frac{\partial T}{\partial r}(r=R)=\frac{Bi}{R}\left(T_w - T|_{r=R}\right). \quad (12)$$

The equations were solved by discretizing the radial derivatives using the orthogonal collocation method [13], and the resulting set of first-order ordinary differential equations constituted an initial-value problem which was integrated using variable-order variable step-size predictor–corrector methods [14].

4. Reactor simulations

Two model reactions will be used for the simulations reported in the present work, the catalytic combustion of ethane and the synthesis of vinyl acetate from acetylene and acetic acid. Both reactions exhibit the need for cooling at the wall to prevent thermal runaway, and can thus illustrate the effects of varying the radial wall heat transfer coefficient. In addition, both reactions have been studied extensively and the kinetics are available in the literature. For both examples, the kinetics and parameter values of the original authors are used, except where explicitly stated. For the sake of brevity, the reader is referred to the original references for these equations and values.

4.1. Example 1: ethane combustion

$$C_2H_6 + 3.5O_2 \rightarrow 2CO_2 + 3H_2O.$$

This reaction was studied by Vortmeyer and Haidegger [1] in a tubular cooled reactor. The reactor had a total length 0.86 m, where the 0.16 m long catalytic section was sandwiched between two inactive particle layers. The catalyst used was PdO on γ-alumina. The tube to particle diameter ratio was 10.

Detailed kinetics are presented in Ref. [1] resulting from extensive laboratory study. Several models were evaluated in Ref. [1], and both

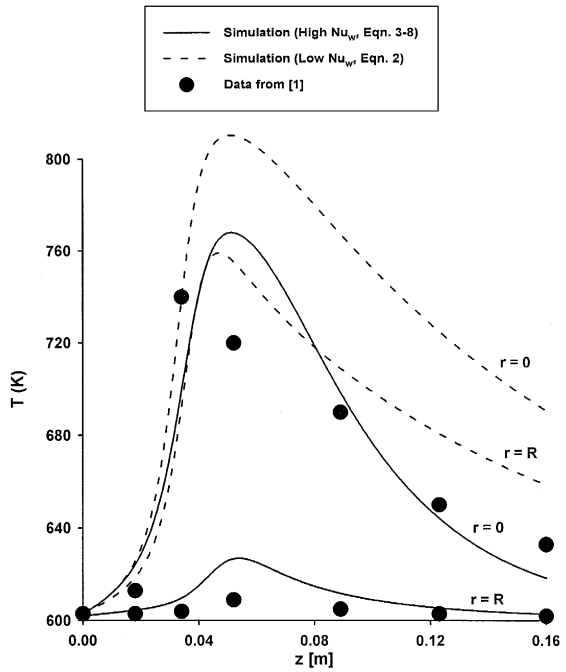

Fig. 4. Simulations of ethane combustion using different Nu_w values: temperature profiles.

those results and the present simulations showed the hot-spot displaced downstream from the measured location. Better agreement with the trends in the data was obtained in our work by adjusting the multiplying factor f_s in the rate expressions from 1.067 to 1.71, for all cases run. The parameter values for the model and correlations were as given in Ref. [1], except that k_r/k_f and Nu_w were evaluated using Eqs. (3)–(8) (or Eq. (2) for comparison), under the conditions of Fig. 2 and Fig. 3. This resulted in values of $k_r/k_f = 10.0$ and $Nu_w = 26$ from Eqs. (3)–(8). Using Eq. (2) gave $Nu_w = 2$.

Representative simulations are presented in Fig. 4 and Fig. 5 for $Re = 25$, an inlet temperature of 603K and a coolant temperature of 601K. In Fig. 4, the temperature profiles simulated using $Nu_w = 26$ are in reasonable qualitative agreement with the data of Vortmeyer and Haidegger [1]. Using $Nu_w = 2$, however, gave simulations that grossly overpredicted the hot-spot magnitude and which could not reproduce the strong temperature differences between the

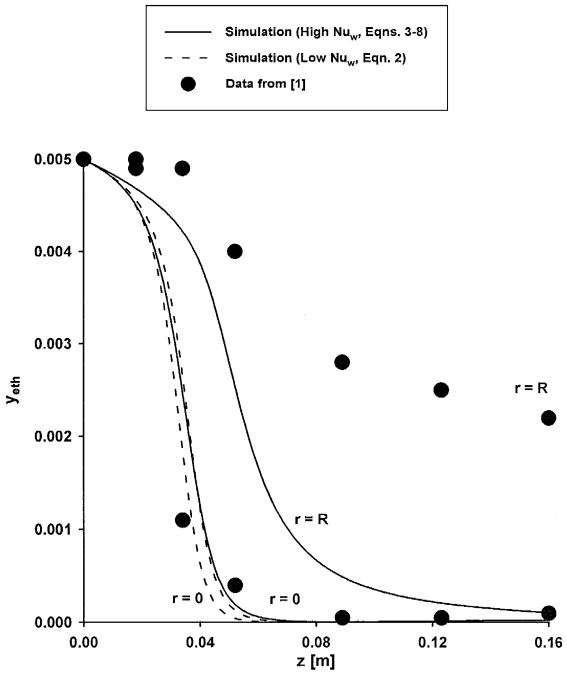

Fig. 5. Simulations of ethane combustion using different Nu_w values: profiles of ethane mass fraction.

bed center ($r = 0$) and the bed wall ($r = R$). In Fig. 5, axial profiles of the ethane mass fraction are given. The profile at the bed center was reasonably well predicted using either value of Nu_w. At the wall, the lower temperatures predicted using $Nu_w = 26$ allowed higher mass fractions of ethane to persist, in qualitative agreement with the data. The higher temperatures predicted using $Nu_w = 2$, on the other hand, forced consumption of the ethane uniformly across the bed radius. Neither value of Nu_w led to good agreement with the $r = R$ data for y_{eth}. Vortmeyer and Haidegger [1] also found the two-dimensional pseudohomogeneous plug-flow model predictions to be lacking. They investigated some more complex models and obtained some improvements in the agreement between model predictions and data.

4.2. Example 2: Vinyl acetate synthesis

$$C_2H_2 + CH_3COOH \rightarrow C_4H_8O_2.$$

This reaction was investigated by Valstar et al. [15] who conducted experimental measurements using a catalyst of zinc acetate on activated carbon. They compared their measurements with two-dimensional reactor calculations, having measured the kinetics and the heat and mass transfer parameters in separate experiments. They found reasonable agreement between predictions and data, and concluded that the value of k_r/k_f had a stronger effect on the simulations than the value of h_w. Recently, this reaction was re-visited by Herskowitz and Hagan [16], who used it as a test case in their study of different one-dimensional fixed bed reactor models.

The kinetics and operating conditions for the present simulations were taken from the study by Herskowitz and Hagan [16], and corresponded to $Re = 58$, a d_t/d_p ratio of 12.4 and a catalyst thermal conductivity giving $k_p/k_f = 26$, presumed to be in cylindrical form. The reactor was 1 m long, with inlet gas composition 60/40 acetylene to acetic acid, and temperature 465.1K. The coolant was at the same temperature as the inlet gas. Under these conditions Eqs. (3)–(8) gave $Nu_w = 19.4$ and $k_r/k_f = 16.4$, while Eq. (2) gave $Nu_w = 4.1$. Valstar et al. [15] obtained $k_r/k_f = 12.8$ and $Bi = 7.22$, leading to

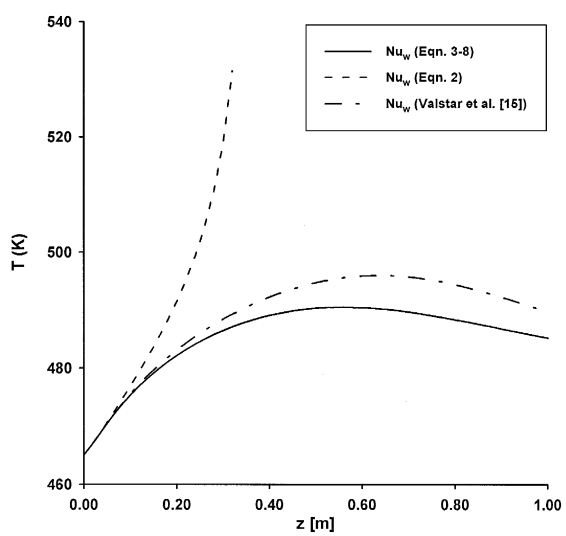

Fig. 6. Simulations of vinyl acetate synthesis using different Nu_w values: temperature profiles.

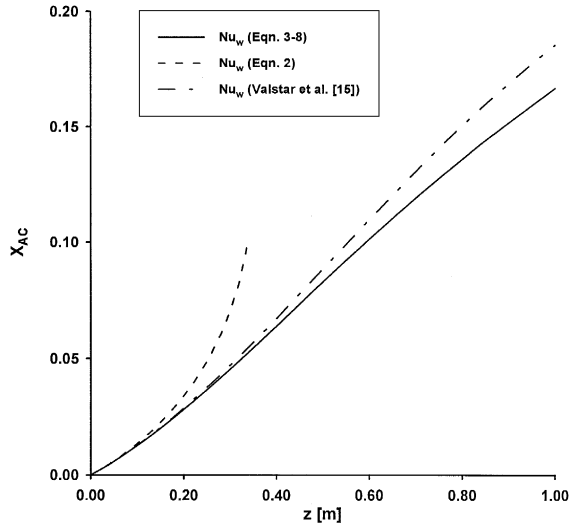

Fig. 7. Simulations of vinyl acetate synthesis using different Nu_w values: acetylene conversion profiles.

$Nu_w = 14.9$. For the simulations reported here, the k_r/k_f value of Valstar et al. [15] was used to avoid confusing the effects of the two parameters. Thus, the effects of changing Nu_w could be studied in isolation.

The results of the simulations are given in Fig. 6 and Fig. 7, showing the axial temperature profiles and the axial conversion profiles of acetylene respectively, both at the bed center ($r = 0$). Clearly the simulations using Nu_w predicted from Eqs. (3)–(8) are in good agreement with the simulations using the measured values of Valstar et al. [15]. Using the low values of Nu_w from Eq. (2), however, led to predictions of runaway, which was not observed experimentally. Although the predictions of the two-dimensional model were not sensitive to relatively small variations of the order of 20–30% in the value of Nu_w for this reaction, changes in the Nu_w value of an order of magnitude or more had a strong effect. Use of an inappropriate correlation could result in differences in the value of Nu_w of this magnitude.

5. Conclusions

From these simulations it can be concluded that for the two reaction examples studied, more realistic results were obtained using the two-dimensional pseudohomogeneous model if the wall heat transfer coefficient was estimated using correlations that accounted for the effects of tube-to-particle diameter ratio, and the thermal conductivity of the catalyst. It should be noted that both reactions were simulated at relatively low values of *Re*. As *Re* increases, all correlations are in good agreement and the issue is of less importance. At low to moderate *Re*, the values of Nu_w can differ by an order of magnitude or more depending on the correlation used.

The main features of the data for both examples were reproduced using a relatively simple model, provided that the better correlation for Nu_w was used. Only marginal improvements would be made by going to complex models with radially-varying velocity and porosity, conduction in the wall, etc. These examples teach us to examine the correlations for reactor heat transfer parameters carefully, before using complicated reactor models.

6. Nomenclature

$\hat{c}_p$:	fluid heat capacity [J/kgK]
d_p:	particle diameter [m]
d_t:	tube diameter [m]
G:	superficial mass flow rate [kg/m^{2}s]
ΔH_R:	reaction enthalpy [kJ/kmol]
h_w:	wall heat transfer coefficient [W/m^{2}K]
k_f:	fluid thermal conductivity [W/mK]
k_p:	particle conductivity [W/mK]
k_r:	effective radial thermal conductivity [W/mK]
k_{rs}:	bed center solid phase radial thermal conductivity [W/mK]
$\bar{k}_{rs}$:	bed average solid phase radial thermal conductivity [W/mK]
M_0:	reactant feed molecular weight
q_r:	radial heat flux [W/m^2]
R:	tube radius [m]

r: radial coordinate [m]
$r(X_A, T)$: reaction rate [kmole/m^{3}s]
T: bed temperature [K]
T_0: bed inlet temperature [K]
T_w: coolant temperature [K]
X_A: conversion of species A
z: axial coordinate [m]

6.1. Greek letters

β_f: dimensionless group defined in Eq. (7)
β_s: dimensionless group defined in Eq. (4)
ϵ: fixed bed void fraction
μ: fluid viscosity [Ns/m^2]
τ: fixed bed tortuosity

6.2. Dimensionless groups

Bi: Biot number $(h_w R/k_r)$
Bi_f: fluid phase Biot number $(h_{wf} R/k_{rf})$
Bi_s: solid phase Biot number $(h_{ws} R/k_{rs})$
N_f: defined in Eq. (8)
N_s: defined in Eq. (5)
Nu_{fs}: fluid–solid Nusselt number $(h_{fs} d_p/k_f)$
Nu_w: Nusselt number $(h_w d_p/k_f)$
Nu_{wf}: fluid phase Nusselt number $(h_{wf} d_p/k_f)$
Pe_{rf}: fluid phase radial Peclet number for heat $(G\hat{c}_p d_p/k_{rf})$
Pe_{rh}: Peclet number for heat transfer $(G\hat{c}_p d_p/k_r)$
Pe_{rm}: Peclet number for mass transfer (ud_p/D_r)
Pr: Prandtl number $(\hat{c}_p \mu/k_f)$
Re: Reynolds number (Gd_p/μ)
y_{A0}: inlet mole fraction of reactant A
y_{eth}: mass fraction of ethane

References

[1] D. Vortmeyer and E. Haidegger, Chem. Eng. Sci., 46 (1991) 2651.
[2] C.A. Coberly and W.R. Marshall Jr., Chem. Eng. Prog., 47 (1951) 141.
[3] E. Tsotsas and E.-U. Schlünder, Chem. Eng. Sci., 45 (1990) 819.
[4] J.G.H. Borkink and K.R. Westerterp, Chem. Eng. Sci., 49 (1994) 863.
[5] C.H. Li and B.A. Finlayson, Chem. Eng. Sci., 32 (1977) 1055.
[6] D. Ziólkowski and B. Legawiec, Chem. Eng. Proc., 21 (1987) 65.
[7] J. Tobís and D. Ziólkowski, Chem. Eng. Sci., 43 (1988) 3031.
[8] A.G. Dixon and D.L. Cresswell, AIChE J., 25 (1979) 663.
[9] H. Martin and M. Nilles, Chemie-Ing.-Tech, 65 (1993) 1468.
[10] M.G. Freiwald and W.R. Paterson, Chem. Eng. Sci., 47 (1992) 1545.
[11] A.G. Dixon, Chem. Eng. Comm., 71 (1988) 217.
[12] G.F. Froment and K.B. Bischoff, Chemical Reactor Analysis and Design, Wiley, New York, 1979.
[13] J. Villadsen and M.L. Michelsen, Solution of Differential Equation Models by Polynomial Approximation, Prentice-Hall, Englewood Cliffs, 1978.
[14] L.F. Shampine and M.K. Gordon, Computer Solution of Ordinary Differential Equations, W.H. Freeman, San Francisco, 1975.
[15] J.M. Valstar, P.J. Van Den Berg and J. Oyserman, Chem. Eng. Sci., 30 (1975) 723.
[16] M. Herskowitz and P.S. Hagan, AIChE J., 34 (1988) 1367.
[17] R.A. Colledge and W.R. Paterson, Coll. Papers, Instn. Chem. Engrs. 11th Annual Res. Meeting, Bath, 1984.
[18] D.L. Cresswell, NATO ASI Series E, 110 (1986) 687.
[19] D. Kunii and J.M. Smith, AIChE J., 6 (1960) 71.
[20] D.J. Gunn, Trans. Inst. Chem. Eng., 47 (1969) T351.
[21] R. Bauer and E.-U. Schlünder, Int. Chem. Eng., 18 (1978) 181.
[22] N. Wakao, S. Kaguei and T. Funazkri, Chem. Eng. Sci., 34 (1979) 325.